Journal of Sound and Vibration 329 (2010) 443–456

Contents lists available at ScienceDirect

Journal of Sound and Vibration

journal homepage: www.elsevier.com/locate/jsvi

Synchronization, multistability and basin crisis in coupled pendula

O.I. Olusola [a], U.E. Vincent [b,c,*], A.N. Njah [a]

[a] Department of Physics, University of Agriculture, Abeokuta, Nigeria
[b] Institut für Theoretische Physik, Technische Universität Clausthal, Arnold-Sommer Str. 6, 38678 Clausthal-Zellerfeld, Germany
[c] Department of Physics, Lancaster University, LA1 4YB Lancaster, UK

ARTICLE INFO

Article history:
Received 7 July 2009
Received in revised form
21 September 2009
Accepted 22 September 2009
Handling Editor: M.P. Cartmell
Available online 27 October 2009

ABSTRACT

The synchronization dynamics of two linearly coupled pendula is studied in this paper. Based on the Lyapunov stability theory and Linear matrix inequality (LMI); some necessary and sufficient conditions for global asymptotic synchronization are derived from which an estimated threshold coupling k_{th}, for the on-set of full synchronization is obtained. The numerical value of k_{th} determined from the average energies of the systems is in good agreement with theoretical analysis. Prior to the on-set of synchronization, the *boundary crisis* of the chaotic attractor is identified. In the bistable states, where *two* asymmetric periodic attractors co-exist, it is shown that the coupled pendula can attain multistable states via a new dynamical transition—the *basin crisis* that occur prior to the on-set of stable synchronization. The essential feature of *basin crisis* is that the *two* co-existing attractors are destroyed while new *three* or *more* co-existing attractors of the same or different periodicity are created. In addition, the linear perturbation technique and the Routh–Hurwitz criteria are employed to investigate the stability of steady states, and clearly identify the different types of bifurcations likely to be encountered. Finally, two-parameter phase plots, show various regions of chaos, hyperchaos and periodicity.

1. Introduction

Coupled nonlinear oscillators exhibit rich catalogues of dynamical behaviour including synchronization and multistability of attractors. On the one hand, the phenomena of synchronization are of fundamental importance in the study of biological, physical and technological problems [1–3]. The history of synchronization dates back to the Huygens discovery of two synchronizing pendulum clocks in 1673 [4]. However, the seminar work of Pecora and Carroll [5] on the synchronization of identical chaotic systems has led to intensive research activities in this area [1,2,5]. The study of synchronized dynamics derived its motivations from its potential applications in communication systems, time series analysis, modelling brain and cardiac rhythm activity and earthquake dynamics [1,6].

Various types of synchronization phenomena which are based on the degree of interaction among oscillators have been identified by many researchers in the recent time [7,8]. Among these are complete synchronization (CS) [5,6,9]; generalized synchronization (GS) [10]; phase synchronization (PS) [11–13]; lag synchronization (LS) [11]; anticipated synchronization (AS) [14,15] and measure synchronization (MS) [16–18]. Practical applications of synchronized dynamics have been reported by many authors, some of which are in laboratory experiments such as lasers [19], plasmas [20] and solar activities [21] and so on.

Sensitivity to initial conditions is a generic feature of chaotic dynamical systems and in particular, synchronization between two identical chaotic system remains an intriguing problem. For a system of two coupled chaotic systems such as

* Corresponding author. Permanent: Department of Physics, Olabisi Onabanjo University, P.M.B. 2002, Ago-Iwoye, Nigeria.
E-mail addresses: sola_olusola2000@yahoo.com (O.I. Olusola), u.vincent@tu-clausthal.de (U.E. Vincent), njahabdul@yahoo.com (A.N. Njah).

0022-460X/$ - see front matter © 2009 Elsevier Ltd. All rights reserved.
doi:10.1016/j.jsv.2009.09.030

$\dot{x}_{1,2} = f_{1,2}(x_{1,2})$, where the overdot represents differentiation with respect to time, t, $x_{1,2}$ are state space variables for systems 1 and 2, $f_{1,2}$ being the corresponding nonlinear functions, synchronization in a direct sense implies that $|x_1 - x_2| \to 0$ as $t \to \infty$. When this occurs, the coupled systems are said to be completely synchronized [2,7,6,9]. Complete synchronization therefore implies a perfect locking of chaotic trajectories in the phase space.

The subject of synchronized dynamics has been a topic of numerous papers, most of which have been demonstrated theoretically [22–24], numerically [25–34] and experimentally [35,36] for several systems. In particular the authors in [26,28,36–41] have shown that the chaotic pendulum is a physically realizable system that exhibits the spectrum of temporal chaotic phenomena [37–39], including control [40,41] and intermittent synchronization [26,28,35,36]. The persistent intermittent synchronization in coupled pendulums as reported by Baker et al. [26,28,35,36], however, occur due to the type of coupling employed in their investigations. In Refs. [26,28,35,36], the two pendulums were coupled linearly through their velocity coordinates. The model could describe a resistively coupled chaotic Josephson junctions as in Ref. [31]. Indeed, the type and topology of coupling may differ and any specific choice of coupling scheme would determine the synchronization outcome. Here, we show that full/complete synchronization can be realized between linearly coupled chaotic pendulum—when the coupling configuration is in the displacement coordinates. Our model employs the spring-type coupling that could exist between interacting particles and has been used (together with the Lernard-Jones potential) to describe interactions among the manomers for single DNA molecule in Brownian dynamics simulations as well as in polyelectrolyte brusches and ssDNA molecules [42–44]. Very recently [45], we employed this kind of linear feedback to study synchronization phenomena in mutually coupled double-wells Duffing oscillators (DDOs) exhibiting cross-well chaos [46]. We showed that the coupled DDOs achieved complete synchronization when the coupling strength was increased beyond a critical value. We also reported that the oscillators in their bistable states undergo basin bifurcations in which multistable states are reached as additional attractors are induced in the phase space; and hence one could find $n+q(n \geq 2, q \geq 1)$ basins of attraction for the co-existing attractors for a given set of parameters. Indeed, the universality of the results that we presented in Ref. [45] and the underlying mechanism are questions that were not treated. Similarly, the synchronization criteria were not theoretically considered. Thus, it would be fundamentally significant and instructive as well to treat these questions and investigate further how attractors are induced and also identify the dynamical mechanism of this phenomenon in the coupled DDO's and other bistable oscillators.

The co-existence of two (bistability) or more (multistability) attractors in phase space are phenomena that have been proven to exist in many fields of science. For instance, Feudel et al. [47–50] demonstrated the phenomenon of multistability in discrete systems using the coupled logistic maps, while Vadivasova et al. [51] extensively demonstrated the sequence of bifurcation scenario leading to multistable state in coupled Rössler systems. In Ref. [52], Neuman et al. reported the coexistence of synchronous and asynchronous motion in quasiperiodically driven logistic maps and also observed an interior crisis-like transitions characterized by a change in the speed of the growth of the attractor size. In particular, as a control parameter varies, attractors may appear, disappear or change stability through different bifurcations. The bifurcations of attractors, in most cases, are associated with the transformations of their basins of attraction so that their structures may be very complicated, or even fractal.

In the present paper, we extend our previous study in Ref. [45] to the coupled chaotic pendula. First, we employ the Lyapunov stability theory and the LMI [53] to obtain some necessary and sufficient conditions for the occurrence of stable and global synchrony. We examine in detail the synchronization behaviour and show that the tumbling chaotic attractor of the pendulum is destroyed in an exterior crisis during the transition to synchronization. We also report the existence of multistable states prior to the on-set of stable synchronized dynamics and further show that the transition to multistable states is a direct consequence of a new dynamical transition which we term *basin crisis*. Crises phenomena have been reported earlier in the literature basically for uncoupled oscillators (see for example Refs. [54,55]). They are usually related to sudden changes in chaotic attractors with parameter variation and such changes are caused by the collision of the chaotic attractor with an unstable periodic orbit or, equivalently its stable manifold [56]. The reader may refer to Refs. [56,57] for comprehensive description of different roots to chaos as well as the three types of crisis that have been reported in the literature. Recent studies have also identified the crisis event in coupled oscillators when the oscillators transit from nonsynchronous to synchronous state [9,30,32,33,58]. The *basin crisis* which we found here is associated with the destruction of co-existing periodic attractors and the creation of different co-existing periodic attractors of the same or of different periodicity during the transition to synchronization; and has not been reported previously in the literature to the best of our knowledge. This phenomenon could be generic in bistable oscillators. The rest of this paper is structured as follows: In Section 2 we give a brief description of the system. Sections 3 is devoted to the stability analysis and synchronization criteria; while in Section 4, we give some numerical results on synchronization dynamics. We discuss basin crisis and multistability in Section 5 and summarize the paper with some concluding remarks in Section 6.

2. Model description

Mathematical model of the oscillator that we study is assumed in the form of a second order nonautonomous differential equation [46]

$$\ddot{x} + h\dot{x} + \frac{dV}{dx} + f(g, \omega, t) = 0, \tag{1}$$

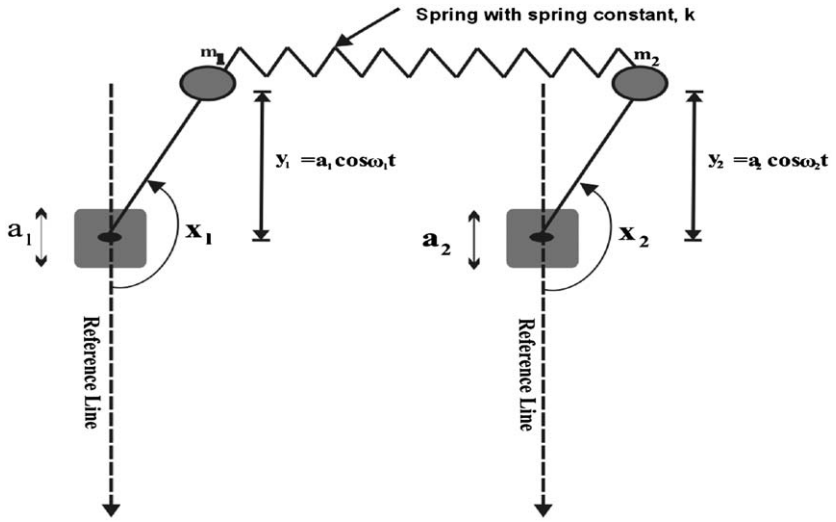

Fig. 1. Schematics of two coupled periodically driven pendula interacting via the elastic spring with spring-constant, k. Notice that each of the pendulum of mass m_i $(i=1,2)$ is given a displacement x_i $(i=1,2)$ in anti-clockwise direction as shown.

where x represents the displacement from equilibrium position, h is the damping coefficient, $f(g,\omega,t)$ is the periodic function of time with the period $T=2\pi/\omega$, g and ω are the amplitude and frequency of external forcing, respectively; and $V(x)$ is the periodic potential given by

$$V(x)=1-\cos x. \tag{2}$$

$V(x)$ is minimum at $x=2n\pi$ and maximum at $x=(2n-1)\pi$, $(n=0,1,2\ldots)$. When two of such system (1) interact with each other through a specific coupling, the potential (2) is perturbed and the potential governing such a coupled system is of the form

$$V(x_{1,2})=2-(\cos x_1+\cos x_2)+\frac{k}{2}(x_1-x_2)^2, \tag{3}$$

where the last term is the coupling term, k being the coupling parameter which determines the strength of the coupling. With $k=0$ Eq. (3) describes the potential for two uncoupled systems exhibiting both regular and chaotic dynamics when a strong periodic forcing is applied. In this case it is obvious that the potential has equilibrium at $(x_1,x_2)=(0,0)$ and symmetrical about this point. With $k\neq 0$, the equilibrium as well as the symmetry is changed and the dynamics is thus expected to be even richer and more interesting.

The following coupled oscillators can be modelled by the potential (3): (i) coupled periodically driven pendula, (ii) coupled parametrically excited pendula and (iii) coupled Duffing oscillators. These oscillators have been studied extensively in the uncoupled state. A comparative study of their dynamics has been presented by Szemplinska and Tyrkiel [46]. They showed that *tumbling chaotic motion* consisting of an irregular combination of rotations and oscillations in this class of oscillators is preceded by the two and only two co-existing periodic attractors, which are simultaneously annihilated prior to period-doubling cascade scenario. Indeed, the results which we present here have been verified for this class of oscillators; and could be verified also for autonomous bistable oscillators.

The system that we study here consists of two mutually coupled identical periodically driven pendula (see Fig. 1) described by the following set of second order differential equations [46]

$$\ddot{x}_{1,2}+h\dot{x}_{1,2}+\frac{\mathrm{d}V(x_{1,2})}{\mathrm{d}x}=a_{1,2}\cos(\omega_{1,2}t), \tag{4}$$

where the state variables $x_{1,2}$ denote the rotation angle in anti-clockwise direction from the equilibrium position of coupled pendula which consists of rigid massless rods carrying point masses (at the ends) with h being damping parameter and $a_{1,2},\omega$ represent amplitude and angular frequency of forcing, respectively. System (4) could be used to model two coupled Josephson junctions [31,59].

3. Stability and synchronization criteria

In this section, we would employ the Lyapunov stability theory and linear matrix inequalities to obtain some sufficient criteria for global and full synchronization. Each isolated oscillator with common periodic-driving force can be re-written

in the autonomous form as follows:

$$\dot{x}_{1,2} = y_{1,2},$$

$$\dot{y}_{1,2} = -hy_{1,2} - \sin x_{12} + a\cos\omega t. \tag{5}$$

Equivalently in a compact vector form, we can write (5) as

$$\dot{\mathbf{X}}_1 = \mathbf{A}\mathbf{X}_\mathbf{1} + \mathbf{f}(\mathbf{X}_\mathbf{1}) + \mathbf{m}(t) - \mathbf{u}, \tag{6}$$

$$\dot{\mathbf{X}}_2 = \mathbf{A}\mathbf{X}_\mathbf{2} + \mathbf{f}(\mathbf{X}_\mathbf{2}) + \mathbf{m}(t) + \mathbf{u}, \tag{7}$$

where $\mathbf{u} = \mathbf{K}(x_1 - x_2)$ is the linear feedback controller arising from the perturbed potential and $\mathbf{K} \in \mathbf{R}^{2\times 2}$ is a constant control matrix. $\mathbf{X}_{\mathbf{1,2}} = (x_{1,2}, y_{1,2})^{\mathrm{T}} \in \mathbf{R}^2$, $\mathbf{A} = \begin{pmatrix} 0 & 1 \\ 0 & -h \end{pmatrix}$, $\mathbf{f}(\mathbf{X}_{\mathbf{1,2}}) = \begin{pmatrix} 0 \\ -\sin x_{1,2} \end{pmatrix}$ and $\mathbf{m}(t) = \begin{pmatrix} 0 \\ a\cos\omega t \end{pmatrix}$. The synchronization error is defined as the difference between the relevant dynamical variables and it is given by

$$\mathbf{e} = \mathbf{X}_\mathbf{1} - \mathbf{X}_\mathbf{2}. \tag{8}$$

By subtracting Eq. (7) from Eq. (6) and using the definition in Eq. (8), one readily obtain:

$$\dot{\mathbf{e}} = (\mathbf{A} - 2\mathbf{K} + \mathbf{G})\mathbf{e}, \tag{9}$$

where

$$\mathbf{G} = \begin{pmatrix} 0 & 0 \\ g(x_1, x_2) & 0 \end{pmatrix}, \quad g(x_1, x_2) = -\frac{(\sin x_1 - \sin x_2)}{x_1 - x_2}. \tag{10}$$

In the absence of the control matrix, $\mathbf{K}$, Eq. (9) would have an equilibrium at $(0, 0)$. If appropriate $\mathbf{K}$ is chosen such that the equilibrium is unchanged, then the synchronization problem would reduced to that of achieving asymptotic stability of the zero solution of the error system (9). Synchronization in a direct sense implies that with the appropriate choice of coupling matrix, any set of initial conditions $\mathbf{X}_1(0)$ and $\mathbf{X}_2(0)$ satisfy

$$\lim_{t\to\infty} \|\mathbf{e}\| = \lim_{t\to\infty} \|\mathbf{X}_\mathbf{1} - \mathbf{X}_\mathbf{2}\| = 0, \tag{11}$$

where $\|.\|$ represents the Euclidean norm of a vector.

Next, by using stability theory on time varied systems, we derive sufficient criteria for global chaos synchronization in the sense of the error system (9). The following Lemma shall be applied to the main theorem of this paper which is related to the general control matrix

$$\mathbf{K} = \begin{pmatrix} k_{11} & k_{12} \\ k_{21} & k_{22} \end{pmatrix} \in \mathbf{R}^{2\times 2}. \tag{12}$$

Lemma 1. *For $g(x_1, x_2)$ defined by* (10)*, the inequality*

$$|g(x_1, x_2)| \le 1 \tag{13}$$

holds.

Proof. By the differential mean-value theorem we have

$$\sin x_1 - \sin x_2 = (x_1 - x_2)\cos\phi, \quad \phi \in (x_1, x_2) \text{ or } \phi \in (x_2, x_1), \tag{14}$$

so,

$$g(x_1, x_2) = -\frac{(\sin x_1 - \sin x_2)}{x_1 - x_2} = -(\cos\phi), \tag{15}$$

and hence the inequality (13) holds. □

Theorem 1. *If there exists a symmetric positive definite matrix $\mathbf{P} = \begin{pmatrix} p_{11} & p_{12} \\ p_{12} & p_{22} \end{pmatrix}$ and a coupling matrix as defined in Eq.* (12) *such that*

$$\Omega_1 = -2p_{11}k_{11} - k_{21}|p_{12}| + p_{12} < 0, \tag{16}$$

$$\Omega_2 = p_{12}(1 - 2k_{12}) - p_{22}(2k_{22} + h) < 0, \tag{17}$$

$$4\Omega_1 \cdot \Omega_2 > [|p_{11}(1 - 2k_{12}) - p_{12}(2k_{11} + 2k_{22} + h) - 2k_{21}p_{22}| + p_{22}]^2 > 0, \tag{18}$$

then the coupled systems (6) *and* (7) *achieve complete synchronization.*

Proof. Let us assume a quadratic Lyapunov function of the form:

$$V(\mathbf{e}) = \mathbf{e}^{\mathrm{T}}\mathbf{P}\mathbf{e}, \tag{19}$$

where $\mathbf{P}$ is a positive definite symmetric matrix as defined earlier. The derivative of the Lyapunov function with respect to time, t, along the trajectory of the error system (9) can be expressed as

$$\dot{V}(\mathbf{e}) = \dot{\mathbf{e}}^{\mathrm{T}}\mathbf{P}\mathbf{e} + \mathbf{e}^{\mathrm{T}}\mathbf{P}\dot{\mathbf{e}}. \tag{20}$$

Substituting Eq. (9) into the system (20), we have

$$\dot{V}(\mathbf{e}) = \mathbf{e}^{\mathrm{T}}[(\mathbf{A} + \mathbf{G}(t) - 2\mathbf{K})^{\mathrm{T}}\mathbf{P} + \mathbf{P}(\mathbf{A} + \mathbf{G}(t) - 2\mathbf{K})]\mathbf{e}. \tag{21}$$

$\dot{V}(\mathbf{e})$ is negative definite if

$$\gamma = [(\mathbf{A} + \mathbf{G}(t) - 2\mathbf{K})^{\mathrm{T}}\mathbf{P} + \mathbf{P}(\mathbf{A} + \mathbf{G}(t) - 2\mathbf{K})] < 0 \quad \forall t \geq 0. \tag{22}$$

According to Lyapunov stability theory on the linear time-varied system, the inequality in (22) represents a sufficient condition for global asymptotic stability of the linear time-varied error system (9) at the equilibrium point. With $\mathbf{A}, \mathbf{K}, \mathbf{P}, \mathbf{G}$ as defined earlier, Eq. (22) thus becomes

$$\gamma = \begin{pmatrix} \eta_{11} & \eta_{12} \\ \eta_{12} & \eta_{22} \end{pmatrix}, \tag{23}$$

where $\eta_{11} = -4p_{11}k_{11} + 2p_{12}(1 - \beta g - 2k_{21})$, $\eta_{12} = p_{11}(1 - k_{12}) - p_{12}(2k_{11} + 2k_{22} + h) + p_{22}(1 - \beta g - 2k_{21})$, and $\eta_{22} = 2p_{12}(1 - 2k_{12}) - 2p_{22}(2k_{22} + h)$. Since γ is symmetric, γ is negative definite if and only if

$$-4p_{11}k_{11} + 2p_{12}(g - 2k_{21}) < 0, \tag{24}$$

$$2p_{12}(1 - 2k_{12}) - 2p_{22}(2k_{22} + h) < 0, \tag{25}$$

$$\begin{aligned} &4[p_{12}(g - 2k_{21}) - 2p_{11}k_{11}][p_{12}(1 - k_{12}) - p_{22}(2k_{22} + h)] \\ &- [p_{11}(1 - 2k_{12}) - p_{12}(2k_{11} + 2k_{22} + h) + p_{22}(g - 2k_{21})]^2 > 0, \end{aligned} \tag{26}$$

Since the matrix $\mathbf{P}$ is positive definite, we have $p_{11}p_{22} - p_{12}^2 > 0$. It follows by Lemma 1 that,

$$\begin{aligned} &-4p_{11}k_{11} + 2p_{12}(g - 2k_{21}) \leq -4p_{11}k_{11} - 4p_{12}k_{21} + 2p_{12} \leq 2\Omega_1, \\ &|p_{11}(1 - 2k_{12}) - p_{12}(2k_{11} + 2k_{22} + h) + p_{22}(g - 2k_{21})| \leq |p_{11}(1 - 2k_{12}) - p_{12}(2k_{11} + 2k_{22} + h) - 2p_{22}k_{21}| + p_{22}. \end{aligned}$$

Therefore, for any $t > 0$ the inequalities in (24)–(26) hold if the inequalities in (16) to (18) are satisfied. □

In applications the structure of the synchronization controller should be as simple as possible. The following corollaries give some algebraic synchronization criteria for a few simple controllers, which are obtained from Theorem 1.

Corollary 1. *If a control matrix* $\mathbf{K} = diag\{k_1, k_2\}$ *and a positive definite symmetric matrix* $\mathbf{P} = \left(\begin{smallmatrix} p_{11} & p_{12} \\ p_{12} & p_{22} \end{smallmatrix}\right) > 0$ *are chosen such that*

$$k_1 > \frac{|p_{12}|}{2p_{11}}, \tag{27}$$

$$k_2 > \frac{p_{12} - hp_{22}}{2p_{22}}, \tag{28}$$

$$4[2k_1p_{11} - |p_{12}|][p_{22}(2k_2 + h) - p_{12}] - [p_{11} - p_{12}(2k_1 + 2k_2 + h) + p_{22}]^2 > 0, \tag{29}$$

then the coupled systems (6) *and* (7) *achieve complete synchronization.*

Proof. Inequalities (27)–(29) can be obtained according to inequalities (16)–(18) with $k_{11} = k_1, k_{22} = k_2$ and $k_{12} = k_{21} = 0$. □

Corollary 2. *If a control matrix* $\mathbf{K} = diag\{k, k\}$ *and a symmetric positive definite matrix* $\mathbf{P} = \left(\begin{smallmatrix} p_{11} & p_{12} \\ p_{12} & p_{22} \end{smallmatrix}\right) > 0$ *are selected such that*

$$k > \max\left\{\frac{|p_{12}|}{2p_{11}}, \ \frac{p_{12} - hp_{22}}{2p_{22}}\right\} \geq 0, \tag{30}$$

$$\begin{aligned} &16(p_{11}p_{22} - p_{12}^2)k^2 - 8k[2p_{22}|p_{12}| + p_{11}(p_{12} - hp_{22}) - |p_{12}(p_{11} - hp_{12})|] + 4|p_{12}|(p_{12} - hp_{22}) \\ &- [|p_{11} - hp_{12}| + p_{22}]^2 > 0, \end{aligned} \tag{31}$$

then the coupled systems (6) *and* (7) *achieve complete synchronization.*

Proof. By setting $k_1 = k_2 = k$ in the partial synchronization conditions (27)–(28), we obtain inequality (30). For $k > 0$ given by (30), we have

$$[|p_{11} - p_{12}(h + 2k)| + p_{22}]^2 \leq [|p_{11} - hp_{12}| + 2k|p_{12}| + p_{22}]^2. \tag{32}$$

Thus inequalities (31) can be obtained according to the partial synchronization condition (29) with $k_1 = k_2 = k$. Again since $p_{11}p_{22} - p_{12}^2 > 0$, the solution k to the inequality (31) exists. □

Remark 1. If we select $p_{12}=0$ and $p_{11}=p_{22}>0$, the following synchronization criterion can be obtained directly from (31):

$$\mathbf{K}=\{k,k\},\quad k>k_{\text{th}}=\frac{-h+\sqrt{h^2+4}}{4}, \tag{33}$$

where k_{th} is the threshold coupling for full synchronization to occur. In the next section, we would present some numerical simulation results to verify the existence of complete and stable synchronized states.

4. Synchronization dynamics: numerical results

All the results to be presented here were computed with the following parameter settings: $a_{1,2}=0.6, \omega_{1,2}=0.69$ and $h=0.1$. With these parameters the coupled oscillators in Eq. (4) is in a structurally stable *tumbling chaotic* state consisting of a combination of rotations and oscillations as illustrated by the chaotic attractor shown in Fig. 2. This *tumbling chaos* is the only steady-state chaotic motion in a broad area of the system parameter.

Numerical solutions were obtained using a fourth order Runge–Kutta routine as well as the software *Dynamics* [60]. Here, we observe the dynamics of the system as the coupling strength is progressively increased. The quality of synchronization is measured by examining the behaviour of the average error E, defined in [26,28,45] and given by

$$E=\sqrt{(x_2-x_1)^2+(y_2-y_1)^2}. \tag{34}$$

When the coupled oscillators are synchronized, the error dynamics asymptotically becomes zero. That is, $E\to 0$ as $t\to\infty$.

We begin by choosing a coupling strength $k=0$ and plot the average error, E, against the time, t, as shown in Fig. 3, this corresponds to the uncoupled case for which the systems are free running chaotic oscillators. The error dynamics when $k=0$ shows an irregular pattern that is comparable to the size of the attractor. With a small nonzero coupling, the two systems achieve near synchronization, $E(t)\approx 0$, for a significant interval at the earlier stage of the dynamics and then become unlocked and so on (the figure not shown).

However, with appreciable coupling strength, the two systems begin to readjust and build up correlation. For example, the inset of Fig. 3 shows the time dependence of the synchronization quantity E for three other coupling strengths illustrating stable synchronization. Furthermore, the threshold coupling, k_{th}, above which complete synchronization occurs is important. From direct calculation of Eq. (33), we find that $k_{\text{th}}\approx 0.48$. To confirm this numerically, we employ a recent technique that is based on the average interaction energies of the system [17]. The basic idea is that when the oscillators are synchronized, any microscopic property of the systems are equal. One of such microscopic quantity that we consider here is the average bare energies,

$$h_{1,2}=\frac{1}{2}\int_0^{\mathrm{T}} E_{1,2}(t)\,\mathrm{d}t,$$

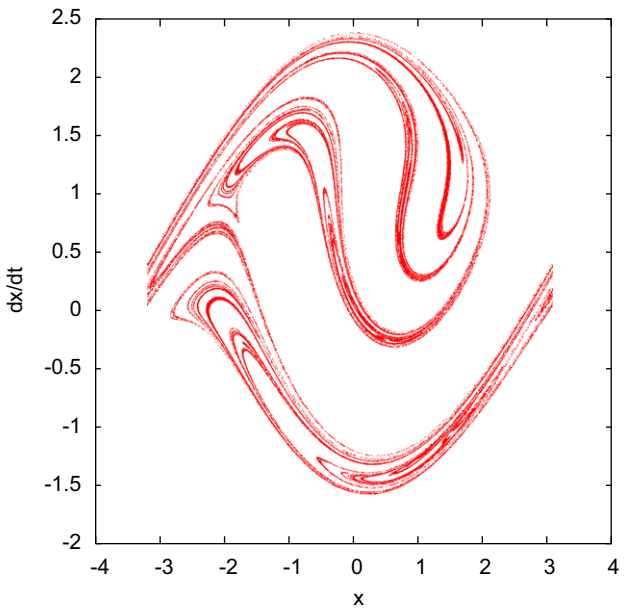

Fig. 2. Poincaré section showing a Tumbling chaotic attractor of the periodically driven pendulum in the $x-y$ ($y=\mathrm{d}x/\mathrm{d}t$) plane for $h=0.1, \omega=0.69, a=0.6$ for $k=0$. This tumbling chaotic attractor consists of a combination of rotation and oscillations; with the rotatory motion dominating [46].

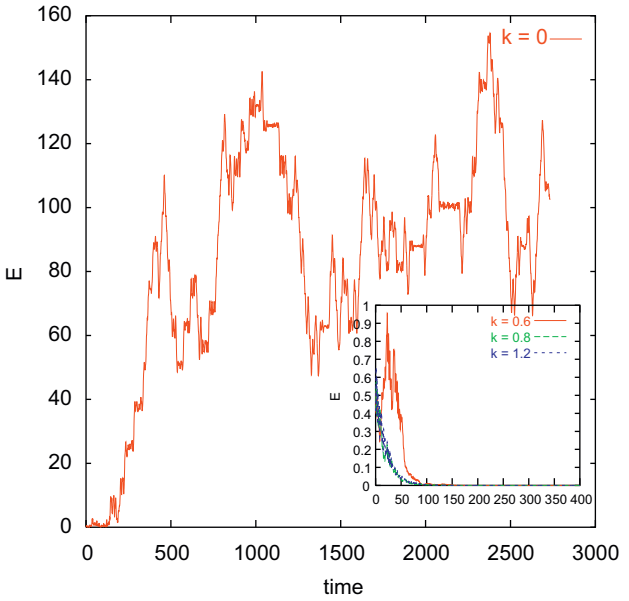

Fig. 3. Time dependence of error dynamics, E for different coupling strength for the coupled periodically forced pendulum. The inset corresponds to $k = 0.6, 0.8$ and 1.2. The other parameters of the system are as in Fig. 2.

where

$$E_{1,2}(t) = \frac{p_{1,2}^2}{2} + V(x_{1,2}), p_{1,2}$$

is the associated momentum and $V(x_{1,2})$ is the potential. In our numerical computation, we account for the transient effect by measuring $h_{1,2}$ after some sufficient initial transients (typically 2000 pre-iterates) has been discarded. We calculated the average bare energies as functions of the coupling strength, k as shown in Fig. 4(a). When k reaches a certain threshold (say, $k_{\text{th}} \approx 0.594$, see the inset which shows the enlargement of the transition point), full synchronization is realized. Above the k_{th} (see inset of Fig. 3(a) for $k > k_{\text{th}}$), the correlation between the oscillators is strongest and the synchronization is stable, indicating that the two oscillators asymptotically approach identical trajectories. This is consistent with the value obtained from Eq. (33) and obviously differs from the persistence intermittency earlier reported in [26,28,35,36]. Further evidence of full synchronization is given in Fig. 4(b). Here, we calculated the average synchronization error,

$$E_{\text{av}} = \frac{1}{T}\int_0^{\text{T}} E(t)\,\text{d}t,$$

where $E(t)$ is given in Eq. (34) and the average interaction energy

$$E_I(t) = \frac{1}{T}\int_0^{\text{T}} E_k(t)\,\text{d}t,$$

where

$$E_k(t) = \frac{k}{2}(x_1 - x_2)^2.$$

Clearly, E_{av} and E_I approaches zero at the critical point and remains stable for $k > k_{\text{th}}$.

5. Multistability and basin crisis

The manner in which attractor basins change with the coupling strength is also an important aspect of the synchronization process that could give further insight into the synchronization behaviour and the dynamics in general. This was reported recently for coupled double well Duffing oscillators in Ref. [45]. It was shown that coupling induced additional attractors (and basins) for some coupling strength prior to the on-set of synchronization. Here, we employ similar numerical procedure to investigate the effect of coupling strength on the attractors and their basins of attraction for the linearly coupled pendula.

Let us consider the coupled periodically driven pendula with the following parameter settings: $\omega = 0.713, h = 0.1, a = 0.6$. For this system parameter in the uncoupled case, two co-existing asymmetric resonant attractors were reported in Ref. [46]. These attractors are found within the narrow band of the frequency and are annihilated prior to the formation of the stable

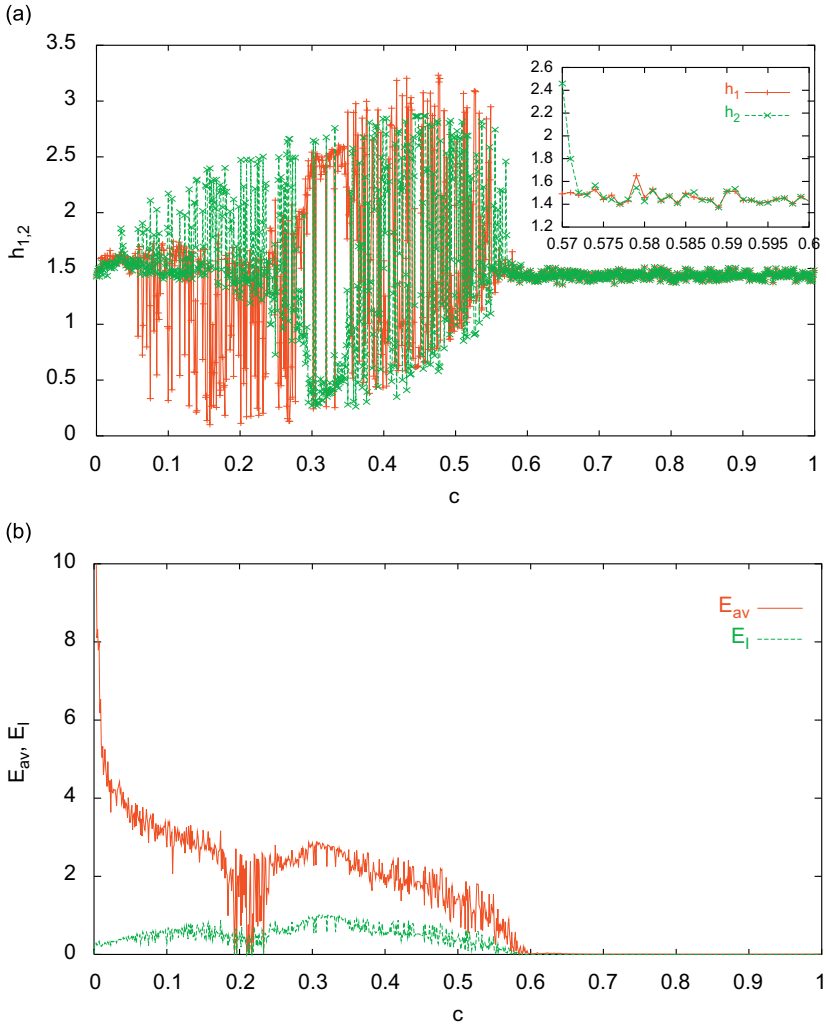

Fig. 4. Synchronization dynamics as functions of the coupling strength. (a) The average bare energies, $h_{1,2}$ *vs* k for the coupled periodically driven pendula for the parameters of Fig. 2. In (b) the average synchronization error, $E_{av} = (1/T)\int_0^T E(t)\,dt$ and the average interaction energies, $E_I = (1/T)\int_0^T E_c(t)\,dt$ are also shown.

tumbling chaotic motion. It should be noted that in the coupled case when synchronization occurs, the coupling term vanishes ($x_1 = x_2$) and the two oscillators are again freely running systems such that two resonant attractors should be found in the subspace, with their corresponding basins characterized with fractal basin boundaries. During the synchronization transition, basin bifurcation occurs leading to different multistable states.

To illustrate the basin bifurcations, we investigate the effects of coupling on the basins of attraction, by visualizing the attractors and their basins of attraction using the software *Dynamics* [60] as employed in [45,46]. We display in Fig. 5, our results. The basins of attraction were numerically generated by selecting a grid of 720×720 points in the region of phase space determined by the rectangle grid of points $(-\pi, \pi) \times (-\pi, \pi)$ which are taken as the initial conditions after 2000 pre-iterates have been discarded considering the long chaotic transients required to allow the system to settle in a stable state. The attractor to which an initial point goes determines the colour assigned to it. In the absence of coupling, (i.e. $k = 0$), the system possesses two co-existing resonant attractors that are asymmetrical to each other (see Fig. 5(a)).

As the coupling is progressively varied (see Fig. 5(b) and (c)), change in the stability of the system occurs as a result of multiple basin bifurcations as we shall show later. The consequences of this bifurcation are (i) the *destruction of the two co-existing T-periodic resonant attractors* and (ii) the *birth (or creation) of new attractors* with the same or different periodicity. For low coupling typically $k < 0.3$, we observed the destruction of the resonant attractors taking place. This is followed by the birth (or creation) of the first set of co-existing attractors at the first bifurcation point ($k \approx 0.3$). For $0.3 \leq k \leq 0.42$, multiple basin bifurcations occur. The number $N = n + q$ ($n \geq 2, q \geq 1$) of attractors that can be created depends on the value of k as well as the initial conditions of the oscillators. To illustrate this, we show in Fig. 5(b) four $2T$- periodic attractors for

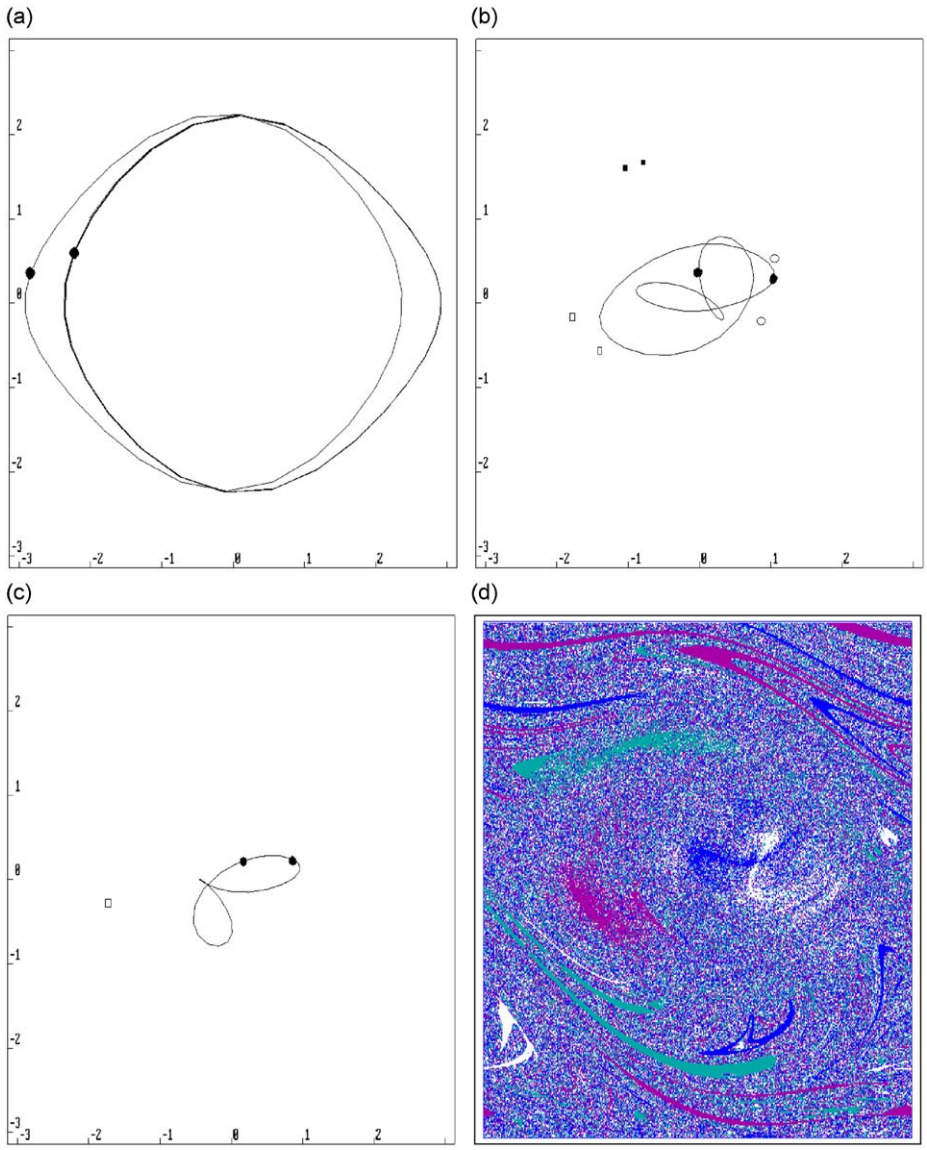

Fig. 5. (a) Two asymmetric coexisting attractors for an uncoupled periodically driven pendulum; (b) four $2T$ periodic attractors for coupled periodically driven pendula ($c = 0.30$); (c) $2T$ periodic attractor coexisting with $1T$ periodic attractor in coupled periodically driven pendula ($c = 0.39$); and (d) the basin structures for the coupled periodically driven pendula for the four co-existing T periodic attractors. The parameters are: $h = 0.1, a = 0.6$ and $\omega = 0.713$.

$k = 0.30$ and in Fig. 5(c) we display three T-periodic attractors for $k = 0.39$. In Fig. 5(d), we also show the basins of attraction of the four attractors shown in Fig. 5(b). Above $k \approx 0.42$, as the oscillators approach the synchronized state, the coupling induced attractors are destroyed completely; while the two resonant attractors re-appear and their basins correspond to that of the uncoupled pendulum . Thus, for a fixed set of the system parameters, an increase in the coupling strength has a significant effect on the number N of the attractors and their basins of attraction. In particular, there is a probability of finding $n+q, n \geq 2, q \geq 1$ basins associated with co-existing attractors in the phase space for the range of parameters studied, implying that coupling induces multistable states in coupled oscillators. For other system parameters and initial conditions, the number n could be greater than the results reported here; and notably, high-dimensional periodic and chaotic attractors could also be found—these could co-exist in phase space as we reported recently for two coupled Duffing oscillators with different potentials [61]. However, the main emphasis here is that multistable states are created as k is progressively increased and are annihilated as the synchronous regime is approached.

It would be significant to examine the stability of the periodic solution in the Poincaré section **dP**. Here, we use linear perturbation analysis as in Refs. [62,63] for Duffing oscillators, to investigate the global bifurcations of this system. The

equation for the perturbed system is given by

$$x_1 = x_{10} + \delta x_1, \quad x_2 = x_{20} + \delta x_2, \quad x_3 = x_{30} + \delta x_3,$$

$$y_1 = y_{10} + \delta y_1, \quad y_2 = y_{20} + \delta y_2, \quad y_3 = y_{30} + \delta y_3, \tag{35}$$

where $\delta x_s, \delta y_s$ and x_{s0}, y_{s0} $(s = 1, 2, 3)$ are small perturbations and steady states, respectively. Thus, using Eq. (35) in (6) and (7) and approximating the sine function with the first two terms in the Taylor series, we obtain the following variational equation

$$\frac{\mathrm{d}\delta\mathbf{F_g}}{\mathrm{d}t} = \mathbf{DV}(f_{g0})\delta\mathbf{F_g}, \tag{36}$$

with

$$\mathbf{DV}(f_{g0}) = \begin{pmatrix} 0 & 1 & 0 & 0 \\ 1 - \frac{1}{2}x_{10}^2 - k & -h & c & 0 \\ 0 & 0 & 0 & 1 \\ c & 0 & 1 - \frac{1}{2}x_{20}^2 - k & -h \end{pmatrix}, \tag{37}$$

where $\mathbf{DV}(f_{g0})$ is the 4×4 Jacobian matrix describing the vector field along the solution $\delta f_g(t)$ and f_{g0} being the equilibrium state. The quadratic and higher order terms are neglected in the perturbations, so that the stability of the periodic motion are determined according to the real parts of the roots of the characteristics equation $\det(\mathbf{DV}(f_{g0}) - I\lambda) = 0$ expressed as

$$\lambda^4 + M_3\lambda^3 + M_2\lambda^2 + M_1\lambda + M_0 = 0, \tag{38}$$

where $M_0 = k^2 - 2k + 1, M_1 = 2h(k-1), M_2 = h^2 - 2 + 2k$ and $M_3 = 2h$ are the coefficients depending on the potential parameters h and k; and $\lambda_i (i = 1, 2, 3, 4)$ are the eigenvalues of $\mathbf{DV}(f_{g0})$. The nature of the roots of Eq. (38) are predicted using Routh–Hurwitz criteria [64] and for different values of $k \in [0.30, 0.50]$. Thus, we obtain a matrix $\mathbf{A}$ associated with (38) given by

$$\mathbf{A} = \begin{vmatrix} M_3 & M_1 & 0 & 0 \\ 1 & M_2 & M_0 & 0 \\ 0 & M_3 & M_1 & 0 \\ 0 & 1 & M_2 & M_0 \end{vmatrix} \tag{39}$$

yielding the following determinants $A_{i's}$:

$$A_1 = M_3 > 0,$$

$$A_2 = M_2M_3 - M_1 > 0,$$

$$A_3 = M_1M_2M_3 - M_0M_3^2 > 0,$$

$$A_4 = M_0M_1M_2M_3 - M_0M_1^2 > 0. \tag{40}$$

With Eq. (40), the Routh–Hurwitz criteria [64] are satisfied, implying that the roots of Eq. (38) have negative real parts. Thus, the system with the given set of parameters k and h can undergo many types of bifurcations namely: saddle-node (sn) (Re$(\lambda_i = 1)$, period-doubling (pd) $(\lambda_i = -1)$, Hopf(H) $(\lambda_i = \omega \pm j\alpha, j^2 = -1)$ bifurcations. Except for Hopf bifurcations, such bifurcations have been reported for a one dimensional pendulum [46]. This analysis allows us to predict how steady state becomes locally unstable and to be aware of the type of bifurcation expected in the system.

The parameter space $(x, \dot{x}, y, \dot{y}, \theta)$ for the full nonlinear system is far too large for a systematic numerical analysis. Here, we employ two-parameter phase diagrams to gain further insight into the global bifurcations in parameter space. Using the software *Dynamics* [60] we fix $h = 0.1$ and display in Fig. 6(a)–(d) different two-parameter phase plots in which several attractors coexist and the prevalence of periodic versus chaotic dynamics. As an example, Fig. 6(a) is a frequency-coupling (i.e. $\omega - k$) phase diagram; here, we observe some feature of Arnol'd tongues in the frequency range of $0.30 \leq \omega \leq 0.375$ and $0.52 \leq \omega \leq 0.78$; indicating the possibility of *mode-locking* phenomenon, wherein stable periodic solution lie on an invariant torus in state space and possesses a period n times the period of oscillation (i.e. $T = 2\pi/\omega$) [65]. It is known that the global bifurcations associated with the Arnol'd tongues include saddle node (sn), period doubling cascades (pd) and sudden chaos [65]. In panels (b) to (d) we depict frequency–amplitude $(\omega - a)$ planes for different coupling strengths $k = 0.30, 0.35$ and 0.42, respectively. Throughout Fig. 6, one can distinguish regions of hyperchaos (dark green), chaos (blue), and quasiperiodicity with period-1 (yellow), period-2 (light green) and period-3 (grey). The dark brown colour corresponds to non-attracting region for which the orbit do not settle to steady state.

As mentioned earlier, the transition to multistable state is a direct consequence of *Basin crisis*. To illustrate this, let us consider the chaotic attractor for the periodically forced pendulum shown in Fig. 2 for $k = 0$. For low coupling, typically below k_{th}, in the nonsynchronized states, Poincaré points of the attractor move on the attractors in an uncorrelated manner,

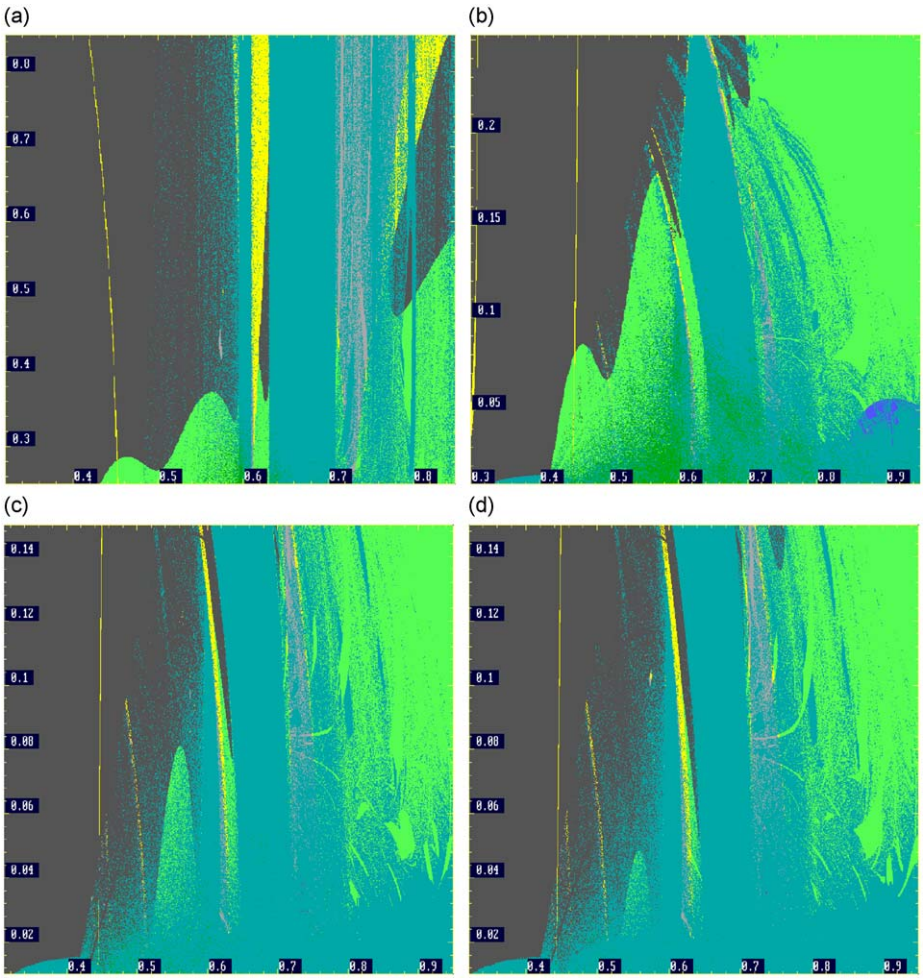

Fig. 6. Two-parameter bifurcation diagram in: (a) $\omega-k$ plane; (b) $\omega-a$ plane for $k=0.30$; (c) $\omega-a$ for $k=0.39$ and (d) $\omega-a$ for $k=0.42$ with the following parameters: $h=0.1, a=0.6, \omega=0.69$. showing regions of hyperchaotic behaviour (dark green), chaos (dark blue), and quasiperiodicity with period-1 (grey), period-2 (light green) and period-3 (yellow) and (brown) region corresponds to nonattraction region. (For interpretation of the references to color in this figure legend, the reader is referred to the web version of this article.)

gradually filling up the entire phase space. For $k=0.35<k_{th}$, shown in Fig. 7, the tumbling chaotic attractor is weakly registered initially, but it is later superposed by uncorrelated Poincaré points due to desynchronous points. We notice that: (i) the *the chaotic attractor has been destroyed*, (ii) the *size has increased* and (iii) the *structure of the distance between it and the basin boundary approaches zero* so that the entire phase space is gradually being filled up with uncorrelated Poincaré points. This is essentially an indicator of a more complex dynamics; and the phenomenon termed *boundary or exterior crisis* of the attractor has been reported earlier as a synchronization transition [9,12,30,32,33]. It is usually attributed to the collision of the attractor with an unstable periodic orbit on its basin boundary or, equivalently its stable manifold [56]. In the synchronized state of mutually coupled oscillators, the chaotic attractor is rebuilt, although there could be residual Poincaré points that do not fall on the main body of the original attractor [32] leaving some spotted appearance in the open parts of the phase space.

Our main interest here is on how this crisis event is manifested in the bistable states of the oscillators. When the oscillators are simulated in their bistable states as illustrated in Fig. 5, we find that the coupling region ($0.3\leq k\leq 0.43$) where multistability is achieved corresponds to the region where boundary crisis of the chaotic attractor occurs. During the transition from bistability to multistability: (i) the *two co-existing T-periodic resonant attractors are destroyed*, (ii) *new attractors are born (or created)* (Hereafter we would refer to the created attractors as *crisis induced attractors*), (iii) the *number of basins increases* and (iv) the *new attractors occupy larger phase-space region*. In *boundary crisis* and *interior crisis*, the topological structure of the attractor is changed. The number of basin does not increase. In the attractor merging crisis, two or more chaotic attractors merge to form one chaotic attractor. The most prominent type (often referred to as sudden chaos) occurs when a chaotic attractor is suddenly destroyed as the parameter passes through its critical value. The transition which we observe here does not fall in any of these three categories and

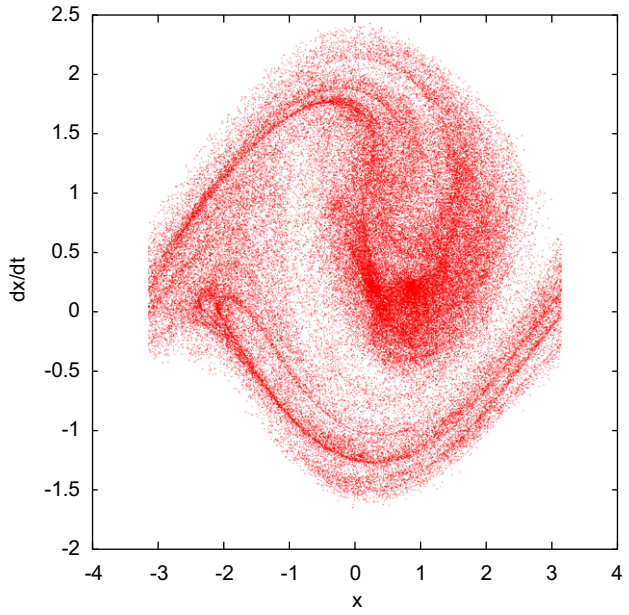

Fig. 7. Trajectories of the attractors in the Poincaré sections illustrating the boundary crisis phenomenon during the transition to synchronized dynamics for the coupled pendulum with periodic forcing for $k = 0.35$. The parameters are as in Fig. 1.

therefore represents a new dynamical transition which we call *Basin crisis* and it is conjecture that it could be generic for coupled bistable oscillators. Notably, a *reverse basin crisis* occurs as the coupled oscillators approach the synchronization region. In this transition, all the *crisis induced attractors* are annihilated and the T-periodic attractors are again created.

6. Summary and conclusions

In summary, we have examined the synchronization and multistability in two linearly coupled chaotic pendulums. The global stability of the synchronized state has been examined using Lyapunov stability theory and linear matrix inequality; and we have obtained some necessary and sufficient conditions for global asymptotic synchronization from which an estimate of the threshold coupling was determined. At low coupling the two oscillators in their chaotic states exhibit transient synchronous behaviour followed by complete synchronization when the coupling strength was increased above a critical value. Numerically, we estimated the threshold coupling for full synchronization to be achieved and found good agreement with theoretical analysis. Prior to the threshold coupling, we identify the *boundary crisis* event in which the chaotic attractor is destroyed and its size increases. In the bistable states, we also found multiple basin bifurcations sequences leading to multistability as the coupled oscillators transit from the nonsynchronized to the synchronized state. In the multistable states different set of attractors co-exist depending on the coupling strength and the initial conditions. The transition to multistability identified as *Basin crisis*, has not been previously reported in the literature, to the best of our knowledge and thus represents a new dynamical transition in coupled oscillators. The essential feature of *Basin crisis* are: (i) the *destruction of the two co-existing attractors* and (ii) the *birth (or creation) of new co-existing attractors with the same or different periodicity*. In the multistable state, there is a probability of finding $N = n + q, n \geq 2, q \geq 1$ attractors in the phase space. The prevalence of these attractors in parameter space were globally examined and we observed that beside chaotic states, hyperchaotic states are possible. We conjecture that this phenomenon could be observed in coupled bistable oscillators and therefore could be further investigated in autonomous dynamical systems like the Lorenz system and the Rössler system.

Acknowledgements

The authors acknowledge the critical comments of anonymous reviewers. UEV is grateful to the Royal Society of London, the British Academy and the Physical Science Research Council, UK for research funding through the Newton International Fellowship scheme. He also acknowledges the Alexander von Humbodlt Foundation, Germany, Prof. Dr. D. Mayer for his hospitality and Olabisi Onabanjo University for granting Research Leave.

References

[1] I.I. Blekhman, *Synchronization in Science and Technology*, AMSE Press, New York, 1988.
[2] A. Pikovsky, M. Rosemblum, J. Kurths, *Synchronization: A Universal Concept in Nonlinear Science*, Cambridge University Press, New York, 2001.
[3] R.F. Nagaev, *Dynamics of Synchronizing Systems*, Springer, Berlin–Heidelberg, 2003.
[4] C. Hugenii, Hollogium Oscillatorium, Apud F. Muguet, France, (1673). English translation: The pendulum clock, Iowa state University press, Ames, 1986.
[5] L.M. Pecora, T.L. Carrol, Synchronization in chaotic systems, *Physical Review Letters* 64 (1990) 821–824.
[6] L. Junge, U. Parlitz, Synchronization of coupled Ginzburg–Landau equations using local potential, *Physical Review E* 61 (2000) 3736–3742.
[7] I.I. Blekhman, A.L. Fradkov, *On General Definition of Synchronization*, World Scientific, Singapore, 2003.
[8] I.I. Blekhman, A.L. Fradhov, O.P. Tomchina, D.E. Bogdanov, Self-synchronization and controlled synchronization: general definition and example design, *Mathematics and Computers in Simulations* 58 (2002) 362–384.
[9] U.E. Vincent, A.N. Njah, O. Akinlade, A.R.T. Solarin, Synchronization of cross-well chaos in coupled duffing oscillators, *International Journal of Modern Physics B* 19 (2005) 3205–3216.
[10] N.F. Rullkov, M.M. Sushchik, L.S. Tsimring, H.D.I. Abarbanel, Generalized synchronization of chaos in directionally coupled chaotic systems, *Physical Review E* 51 (1995) 980–994.
[11] M.G. Rosemblum, A.S. Pikovsky, J. Kurths, From phase to lag synchronization in coupled chaotic oscillators, *Physical Review Letters* 78 (1997) 4193–4196.
[12] G.V. Osipov, A.S. Pikovsky, J. Kurths, Phase synchronization of chaotic rotators, *Physical Review Letters* 88 (2002) (054102(1-4)).
[13] M.G. Rosemblum, A.S. Pikovsky, J. Kurths, Phase synchronization of chaotic oscillators, *Physical Review Letters* 76 (1996) 1804–1807.
[14] H.U. Voss, Anticipating chaotic synchronization, *Physical Review E* 61 (2000) 5115–5119.
[15] M. Kostur, P. Hänggi, P. Talkner, J.L. Meteos, Anticipated synchronization in coupled inertia ratchets with time-delay feedback: a numerical study, *Physical Review E* 72 (2005) (036210(1-6)).
[16] A. Hampton, H.D. Zanette, Measure synchronization in coupled Hamiltonian systems, *Physical Review Letters* 83 (1999) 2179–2182.
[17] X. Wang, M. Zhan, C.-H. Lai, H. Gang, Measure synchronization in coupled φ^4 Hamiltonian systems, *Physical Review E* 67 (2003) (066215(1-8)).
[18] U.E. Vincent, A.N. Njah, O. Akinlade, Measure synchronization in a coupled Hamiltonian systems associated with nonlinear Schroedinger equation, *Modern Physics Letters B* 19 (2005) 737–742.
[19] R. Roy, K.S. Thornburg Jr., Experimental synchronization of chaotic lasers, *Physical Review Letters* 72 (1994) 2009–2012.
[20] C.M. Ticos, E. Rosa Jr., W.B. Pardo, J.A. Walkenstein, M. Monti, Experimental real-time phase synchronization of a paced chaotic plasma discharge, *Physical Review Letters* 85 (2000) 2929–2932.
[21] M. Palus, J. Kurths, U. Schwarz, D. Novotna, I. Charvatova, Is the solar activity cycle synchronized with the inertia motion?, *International Journal of Bifurcation and Chaos* 10 (2000) 2519–2526.
[22] A.N. Carvalho, H.M. Rodrigues, T. Dlotko, Upper semiconductivity of attractors and synchronization, *Journal of Mathematical Analysis and Applications* 220 (1998) 13–41.
[23] P.E. Kloeden, Synchronization of nonautonomous dynamical systems, *Electrical Journal of Differential Equations* 2003 (2003) 1–10.
[24] Y.G. Yu, S.C. Zhang, Adaptive control of uncertain Lu system, *Chaos, Solitons and Fractals* 21 (2004) 643–649.
[25] A.N. Pisarchik, R. James-Reatégui, Intermittent lag synchronization in a driven system of coupled oscillators, *Pramana Journal of Physics* 64 (2005) 503–511.
[26] G.L. Baker, J. Blackburn, H.J.T. Smith, Intermittent synchronization in a pair of coupled chaotic pendulum, *Physical Review Letters* 81 (1998) 554–557.
[27] M. Ding, W. Yang, Observation of intermingled basins in coupled oscillators exhibiting synchronized chaos, *Physical Review E* 54 (1996) 2489–2494.
[28] G.L. Baker, J.A. Blackburn, H.J.T. Smith, A stochastic model of synchronization for pendulums, *Physics Letters A* 252 (1999) 191–197.
[29] S.P. Rajasekar, K. Murali, Coexisting chaotic attractors, their basins of attractions and synchronization of two coupled duffing oscillators, *Physics Letters A* 264 (1999) 283–288.
[30] U.E. Vincent, A.N. Njah, O. Akinlade, A.R.T. Solarin, Phase synchronization of hyperchaotic duffing oscillator, *Journal of the Nigerian Association of Mathematical Physics* 8 (2004) 203–210.
[31] J.A. Blackburn, G.L. Baker, H.J.T. Smith, Intermittent synchronization of resistively coupled Josephson junction, *Physical Review B* 62 (2000) 5931–5935.
[32] U.E. Vincent, A.N. Njah, O. Akinlade, A.R.T. Solarin, Phase synchronization in bi-directionally coupled chaotic ratchets, *Physica A* 360 (2006) 186–196.
[33] U.E. Vincent, A.N. Njah, O. Akinlade, A.R.T. Solarin, Phase synchronization in uni-directionally coupled chaotic ratchets, *Chaos* 14 (2004) 1018–1025.
[34] U.E. Vincent, A. Kenfack, A.N. Njah, O. Akinlade, Bifurcation and chaos in coupled ratchets exhibiting synchronized dynamics, *Physical Review E* 72 (2005) 0562131-8.
[35] H.J.T. Smith, J.A. Blackburn, G.L. Baker, Experimental observation of intermittency in coupled chaotic pendulums, *International Journal of Bifurcation and Chaos Applied Science Engineering* 10 (1999) 1907–1916.
[36] H.J.T. Smith, J.A. Blackburn, G.L. Baker, When two coupled pendulums equal one: a synchronization machine, *International Journal of Bifurcation and Chaos Applied Science Engineering* 13 (2003) 7–18.
[37] D.D. Humieres, M.B. Beasely, B.A. Huberman, A. Libchaber, Chaotic states and routes to chaos in forced pendulum, *Physical Review A* 26 (1982) 3483–3496.
[38] J.A. Blackburn, S. Vik, W. Binruo, H.J.T. Smith, Driven pendulum for studying chaos, *Review of Scientific Instruments* 60 (1989) 422–426.
[39] G.L. Baker, J.P. Gollub, *Chaotic Dynamics: An Introduction*, Cambridge University Press, Cambridge, 1996.
[40] G.L. Baker, Control of the chaotic driven pendulum, *American Journal of Physics* 63 (1985) 832–838.
[41] J. Starrett, R. Tagg, Control of chaotic parametrically driven pendulum, *Physical Review Letters* 74 (1995) 1974–1977.
[42] R. Retkute, J.P. Gleeson, Role of interaction on noise-induced transport of two coupled particles in Brownian ratchet devices, *Fluctuation and Noise Letters* 6 (2006) 263–277.
[43] M. Streek, F. Schmid, T.T. Tuong, A. Ross, Mechanism of DNA separation in entropy trap arrays: a Brownian dynamics simulation, *Journal of Biotechnology* 112 (2004) 79–89.
[44] J.F. Mercier, G.W. Slater, Solid phase DNA amplification: a Brownian dynamics study of crowding effects, *Biophysics Journal* 89 (2005) 32–42.
[45] U.E. Vincent, A.N. Njah, O. Akinlade, Synchronization and basin bifurcations in mutually coupled oscillators, *Pramana Journal of Physics* 68 (2007) 749–756.
[46] W. Szemplinska-Stupnicka, E. Tykiel, Common feature of the onset of the persistent chaos in nonlinear oscillators: a phenomenological approach, *Nonlinear Dynamics* 27 (2002) 271–293.
[47] U. Feudel, C. Grebogi, B.R. Hunt, J.A. Yorke, Map with more than 100 coexisting low-period periodic attractors, *Physical Review E* 54 (1996) 71–81.
[48] U. Feudel, C. Grebogi, Multistability and the control of complexity, *Chaos* 7 (1997) 597–603.
[49] U. Feudel, C. Grebogi, Why are chaotic attractors rare in multistable systems, *Physical Review Letters* 91 (2003) (134102(1-4)).
[50] M.D. Shrimali, A. Prasad, R. Ramaswamy, U. Feudel, Basins bifurcation in quasiperiodic forced coupled systems, *Physical Review E* 72 (2005) (036215(1-8)).
[51] T.E. Vadivasova, O.V. Sosnovtseva, A.G. Balanov, V.V. Astakhov, Phase multistability of synchronous chaotic oscillations, *Discrete Dynamics in Nature and Society* 4 (1999) 231–243.
[52] E. Neuman, I. Shusko, Y. Maistrenko, U. Feudel, Synchronization and desynchronization under the influence of quasiperiodic forcing, *Physical Review E* 67 (2003) (026202(1-15)).
[53] X. Wu, J. Cai, M. Wang, Master–slave chaos synchronization criteria for the horizontal platform systems via linear state error feedback control, *Journal of Sound and Vibration* 295 (2006) 378–387.
[54] C. Grebogi, E. Ott, J.A. Yorke, Crises, sudden changes in chaotic attractors and transient chaos, *Physica D* 7 (1983) 181–200.
[55] C. Grebogi, E. Ott, J.A. Yorke, Chaotic attractors in crisis, *Physical Review Letters* 48 (1982) 1507–1510.

[56] E. Ott, *Chaos in Dynamical Systems*, Cambridge University Press, Cambridge, 2002.
[57] Y. Ueda, *The Road to Chaos—II*, Future University, Hakodate, 2001.
[58] S. Denisov, Collective current rectification, *Physica A* 377 (2007) 429–434.
[59] J. Wang, X. Zhang, G. You, F. Zhou, Transition behaviours in two coupled Josephson junction equations, *Journal of Physics A: Mathematical and Theoretical* 40 (2007) 3775–3784.
[60] H.E. Nusse, J.A. Yorke, *Dynamics: Numerical Exploration*, Springer, New York, 1998.
[61] U.E. Vincent, A. Kenfack, Synchronization and bifurcation structures in coupled periodically forced non-identical duffing oscillators, *Physica Scripta* 77 (2008) (0545005(1-7)).
[62] J. Kozlowski, U. Parlitz, W. Lauterborn, Bifurcation analysis of two coupled periodically driven duffing oscillators, *Physical Review E* 51 (1995) 1861–1867.
[63] A. Kenfack, Bifurcation structure of two coupled periodically driven double-well duffing oscillators, *Chaos Solitons and Fractals* 15 (2002) 205–218.
[64] L. Cesari, *Asymptotic Behaviour and Stability Problems in Ordinary Differential Equations*, Academic Press, London, 1963, pp. 21–24.
[65] R. Mettin, U. Parlitz, W. Lauterborn, Bifurcation structure of the driven van der poll oscillator, *International Journal of Bifurcation and Chaos* 6 (1993) 1529–1555.